

**NASA
Technical
Paper
2262**

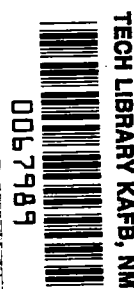
**AVSCOM
Technical
Report
83-B-7**

February 1984

Friction and Wear Behavior of Aluminum and Composite Airplane Skins

Karen E. Jackson

**LOAN COPY: RETURN TO
AFWL TECHNICAL LIBRARY
KIRTLAND AFB, N.M. 87117**





**NASA
Technical
Paper
2262**

**AVSCOM
Technical
Report
83-B-7**

1984

Friction and Wear Behavior of Aluminum and Composite Airplane Skins

Karen E. Jackson

*Structures Laboratory
USAAVSCOM Research and Technology Laboratories
Langley Research Center
Hampton, Virginia*

NASA

National Aeronautics
and Space Administration

**Scientific and Technical
Information Office**

1984

Use of trade names or names of manufacturers in this report does not constitute an official endorsement of such products or manufacturers, either expressed or implied, by the National Aeronautics and Space Administration.

SUMMARY

Experiments were performed to compare the friction and wear behavior of aluminum and composite materials under conditions similar to the loadings experienced by skin panels on the underside of a transport airplane during an emergency belly landing. Small skin specimens were constructed of aluminum, standard graphite-epoxy composite, aramid-epoxy composite, and toughened-resin composites. These specimens were abraded at a range of pressures, abrasive-surface textures, velocities, and fiber orientations. In addition, a temperature-time history was obtained by imbedding thermocouples in one set of specimens and abrading them for a specified time.

Comparisons of the materials were made based on coefficient-of-friction data and the wear rate (defined as the loss of thickness per unit of run time) as a function of the test variables. The composite materials exhibited wear rates 5 to 8 times higher than the aluminum, with the toughened-resin composites having the highest wear rates under identical test conditions. The wear behavior was a linear function of pressure, surface texture, velocity, and fiber orientation. The coefficient of friction of each material was independent of the test variables. The standard graphite-epoxy composite had a coefficient of friction (0.10 to 0.12) approximately half that of aluminum (0.20), whereas the aramid-epoxy and toughened-resin composites had coefficients of friction about the same as aluminum. Results of the temperature tests indicate the temperature of the skin specimens remained fairly constant during the first seconds of abrasion, then increased rapidly in a highly nonlinear manner. Aluminum exhibited the highest rate of increase in temperature and reached the highest temperature of the materials tested during abrasion tests at a specified time.

INTRODUCTION

Composite materials are gaining increased use in the airplane industry because of their excellent mechanical properties, tailorability, and light weight. Much research has been concentrated on composite structures to determine their strength capabilities and to characterize failure mechanisms, damage tolerance, and fatigue life. These efforts have led to an understanding of how composite structures perform under in-flight conditions. In addition, researchers are investigating the response of composite and aluminum structures to dynamic impact loadings. The goal is to evaluate and improve the energy absorption of composite structures, thereby enabling designers to build safer, more crashworthy airplane.

One consideration which can be important in the design of crashworthy airplane is the abrasion and wear behavior of the skin material. In the last 5 years at least a dozen transport airplane have experienced collapse of the landing gear leading to sliding landings on runway surfaces (ref. 1). Typically, these transport airplane slide 4000 to 5000 ft with touchdown velocities of approximately 140 mph. In some sections of the airplane, wear damage to the aluminum skin is considerable, although it is usually repairable. The anticipated increase in the use of composite materials in the airplane industry raises the question of how transport airplane with composite skins would behave under these circumstances as compared with current aluminum construction.

This paper describes an investigation of the friction and wear behavior of small skin specimens under abrasive loading conditions similar to those experienced on the underside of a transport airplane during an emergency belly landing. A test apparatus was designed which used a standard belt sander to provide the sliding surface. The test apparatus was equipped with a load cell capable of measuring the frictional forces developed during abrasion. Small test specimens constructed of aluminum, standard graphite-epoxy composite, aramid-epoxy composite, and toughened-resin composites were tested at a range of pressures, belt velocities, and belt-surface textures. The effects of these test variables on the wear rate and on the coefficient of friction are discussed and comparisons are made between the composite materials and aluminum. The effect of fiber orientation in the composite materials on wear rate was also investigated. In addition, one series of tests was performed in which thermocouples were imbedded in the various test specimens to obtain temperature-time histories during abrasion.

TEST APPARATUS AND PROCEDURES

Equipment

Apparatus.- The apparatus used to perform abrasion tests on composite and aluminum skin specimens is shown in figures 1 and 2. A belt sander fitted with a 6-in. by 48-in. aluminum oxide belt provided the sliding, abrasive surface. Test specimens were held in place by a specimen holder which was attached to the belt sander by a parallelogram arrangement of mechanical linkages. The linkages were pivoted about a back upright such that the specimen holder could be raised from and lowered to the abrading surface. The test specimens fitted into a slight recess in the specimen holder and were held securely in place by a vacuum created behind the specimen by the vacuum pump. (fig. 1).

Figure 2 shows a detailed sketch of the test apparatus in the locked (upper position) and test (lower position) configurations, where the upper position is shown by dashed lines. The specimen holder remained perpendicular to the abrading surface because of the parallelogram linkage arrangement. As the specimen wore, this arrangement kept the load normal to the abrading surface. Loads were applied to the specimen by placing lead weights on a rod attached to the specimen holder. A counterweight was used to offset any load applied to the specimen by the weight of the linkages and the specimen holder.

Instrumentation.- The test apparatus was instrumented with a load cell located in the lower linkage arm (fig. 2). During abrasion test runs the friction force developed between the specimen and the belt produced a tensile force in the lower arm. The strain induced by this tensile force was converted by the load cell into an electrical signal which was amplified and filtered through a 10-Hz low-pass filter. The signal was then fed to a two-channel strip-chart recorder to provide a force data trace. This force measurement was used to calculate the friction and normal forces from a static analysis of the specimen holder given the applied load, the angle of inclination of the linkage arms, and the holder dimensions.

The test apparatus was also instrumented with a limit switch (fig. 1). The limit switch triggered an event marker on the strip-chart recorder when the test specimen was lowered to the abrading surface at the start of a test run. When the run was complete, the test specimen was raised, the limit switch was released, and

the event marker returned to its original position. The test run time was then determined by counting the length of travel of the event marker and dividing that value by the chart speed.

Procedure

Prior to testing, all pertinent data such as test specimen thickness and mass and test parameters such as load, belt velocity, and belt texture (indicated by grit size) were recorded. Test specimens were abraded for approximately 5 sec. This length of time was sufficient to get an adequate force data trace, yet short enough to prevent clogging of the belt with debris. Following the test, the test specimen mass was measured and recorded. The specimen holder and linkage assembly was then adjusted horizontally to allow for another test run with a new specimen on an unused track of the belt. In this manner, three abrasion tests were performed per belt with each test being run on a new belt surface.

Specimens

A schematic drawing of a typical abrasion test specimen is shown in figure 3. Thicknesses of the specimens varied, depending on the material, and ranged from 0.20 to 0.30 in. A 45° bevel on the front edge of the specimen helped to smooth the initial contact of the specimen to the abrading surface. Figure 3 also lists the types of aluminum and composite materials tested, giving the lay-up of each of the composite specimens. Aluminum 2024-T4 is a readily available stock aluminum. The T300/5208¹ is a standard commercial graphite-epoxy composite in wide use today. Kevlar 49/934² is a popular aramid-epoxy composite, also commercially available. Three additional graphite-epoxy materials (T300/BP-907, T300/Fibredux 920, and T300/Ciba 4³) chosen for testing are toughened-resin composites. The epoxy resin in these three materials has been modified by additives and chemical formulations to make them tougher and more damage tolerant. Typically these resin systems have higher ultimate tensile strengths and higher ultimate strains than the 5208 epoxy resin. Additional information on these materials is given in reference 2, which describes a study of toughened-resin composites for impact damage tolerance.

The test specimens used to evaluate the effect of fiber orientation on wear rate were constructed from a 24-ply, unidirectional panel of AS4/3502⁴ graphite-epoxy composite material. A set of eight specimens was cut from the panel such that all fibers in the test specimen were oriented at 0° (parallel) to the sliding direction. Another set of eight specimens was cut having fibers oriented at 15° to the sliding direction. In all, specimens having fibers oriented at 0°, 15°, 30°, 45°, 60°, and 90° to the sliding direction were constructed from the unidirectional panel and used for abrasion testing.

¹Thornel 300 (T300) graphite fiber is manufactured by Union Carbide Corporation; 5208 epoxy resin is manufactured by Narmco Materials, a subsidiary of Celanese Corporation.

²Kevlar 49 aramid fiber is manufactured by E. I. du Pont de Nemours & Co., Inc.; 934 epoxy resin is manufactured by Fiberite Corporation.

³BP-907 epoxy resin is manufactured by American Cyanamid Corporation; Fibredux 920 and Ciba 4 epoxy resins are manufactured by Ciba Geigy Co. Ciba 4 is a specially prepared epoxy resin not available commercially.

⁴AS4/3502 graphite-epoxy composite is a prepreg manufactured by Hercules Incorporated.

Parameters

Pressure conditions.- The effect of pressure on specimen wear rate was determined for each material at pressures of 2.0, 3.2, and 4.8 psi. Typical loading conditions on the skin panels of a transport airplane during an emergency belly landing would fall in the range of 2.0 to 5.0 psi. These test pressures were achieved by placing 5-, 8-, and 12-lb lead weights on the rod above the specimen holder normal to the test specimen. All tests to determine the effect of load on friction and wear behavior were performed on No. 36 grit aluminum oxide belts at a belt velocity of 36.4 mph.

Surface texture.- Standard 6-in. by 48-in. aluminum oxide abrasive belts with grit sizes ranging from No. 36 to No. 60 were used to simulate a runway surface. This range of grit sizes was selected based on the average surface texture depths of these belts as measured with the grease sample technique (ref. 3), which has evolved as a method of classifying runway surfaces. This technique, illustrated in figure 4, involves marking a constant width on the surface to be tested and spreading a known volume of grease evenly within the marked region, filling the crevices and covering as much of the surface as possible. The volume of grease used divided by the surface area covered is the average surface texture depth.

Figure 5 (from data in ref. 4) shows the various surface types and classes of runways and the average surface texture depths measured for runways within each class. The texture depth range of 0.01 to 0.02 in., shown as the shaded region in figure 5, is considered typical for runway surfaces. Therefore, to simulate a runway surface, abrasive belts with texture depths in or near this range were desired; as shown in figure 6, belts having surface textures within or near the 0.01- to 0.02-in. range were those with No. 36, No. 40, No. 50, and No. 60 grit sizes.

The effect of surface texture on specimen wear rate was determined for each type of test specimen using belts with the grit sizes given above. During these tests, the pressure applied to the specimen was 3.2 psi (8 lb load) and the belt velocity was 36.4 mph, so the only variable in the tests was surface texture.

Velocity range.- Typical touchdown velocities of transport airplane are approximately 140 to 160 mph. This high velocity range was unattainable with the motor drive system of the belt sander. However, by altering the pulley ratios, a range of velocities was achieved for testing. Tests at 16.0, 36.4, 52.0, and 68.0 mph were performed on each test material at a pressure of 3.2 psi using a No. 36 grit belt.

Fiber orientation.- The effect of fiber orientation on wear rate was determined by conducting a series of tests on graphite-epoxy composite specimens having fiber orientations of 0°, 15°, 30°, 45°, 60°, and 90° with respect to the sliding direction. Tests on these specimens were conducted at 3.2 psi normal pressure using a No. 50 grit belt.

Temperature.- Four iron-constantan type J thermocouples were imbedded 0.080 in. into the thickness of each specimen on the side opposite the abrading surface. These specimens were abraded on a No. 36 grit belt under a 3.2-psi pressure at a belt velocity of 36.4 mph for approximately 20 sec. Temperature readings from each of the four thermocouples were taken every 4 sec during the runs. Temperature-time histories for each of the six test materials were obtained from these data.

RESULTS AND DISCUSSION

The general appearance of the abraded wear surface and the wear debris are shown in figure 7 for typical Kevlar, graphite-epoxy, and aluminum specimens. The wear surface of the aluminum specimens contained thin, evenly spaced grooves along the direction of sliding. Aluminum wear debris consisted of small particles having a powder-like texture. The graphite-epoxy specimens exhibited a wear surface with long grooves similar to the aluminum specimen, although the graphite-epoxy surfaces were smoother and the grooves were not quite as deep. Wear debris from these specimens consisted mainly of fine particles interspersed with some pieces of broken fibers. The Kevlar specimens were unique in both the appearance of the wear surface and in the wear debris. The wear surface of a Kevlar specimen (fig. 7) showed the characteristic groove markings, although the grooves were smooth and irregularly spaced. In addition, areas of the surface were covered with rough patches where fibers had been shredded from the surface. As the fibers were pulled from the surface of the specimen they tended to break apart and form a fluffy clump of material having a texture resembling cotton. During test runs this clump of wear debris would collect at the back edge of the specimen, grow, and then completely detach from the specimen.

In the following sections, the effects of independently varying four test variables (pressure, surface texture, belt velocity, and fiber orientation) on the wear behavior of six different specimens are discussed and comparisons are made between materials. In particular, the discussions concentrate on how the specimen wear rate is affected by the test variables. The wear rate is defined to be the reduction in specimen thickness per unit of run time and is calculated from the following equation:

$$\text{Wear rate} = \frac{(1 - m_f/m_i)h_i}{t_r}$$

where

h_i initial thickness

m_i initial mass

m_f final mass

t_r run time

Thus, wear rate was computed in dimensions of inches per second. Wear rate was chosen as the dependent variable for this investigation as opposed to wear volume or wear volume per time. Although all specimens were abraded for approximately 5 sec, there was no precise control on run time. Therefore, some specimens were abraded for 4.7 sec, some for 5.2 sec, and so forth. Because the wear behavior is described in terms of the specimen wear rate, the results become independent of the minor variations in run time. In addition to the variations in wear rate, comparisons between the six test materials are made based on the coefficient-of-friction data and on the temperature-time histories.

Wear Behavior

Effect of pressure.- The specimen wear rate as a function of normal pressure, shown in figure 8, exhibited a linear relationship for the six materials tested. Each data point on the graph represents the average of two or three individual tests. A least-squares linear curve fit was made through the points. These results agree with the findings of several other investigations, which report a similar linear relationship between wear of materials and applied load (refs. 5 to 7).

The aluminum 2024-T4 specimen exhibited the lowest overall wear rate and the smallest increase in wear rate with pressure of all the materials tested. The standard graphite-epoxy (T300/5208) and the Kevlar 49/934 specimen had the lowest wear rates of the composite materials tested. The three toughened-resin composites showed the highest wear rates at the pressures tested, with the T300/Fibredux 920 material being the highest as well as having the largest increase with pressure. The most important result of this particular test was not the linear nature of the curves but the large difference in wear rates between the materials tested, as illustrated in figure 9. The wear rates for each material at the 3.2-psi pressure are plotted as a bar chart. The wear rates of the composite materials range from about 5 to 8 times higher than that of the aluminum. The increase in wear rate from the standard graphite-epoxy composite to the toughened-resin composite is also illustrated. Since the same fiber (T300) was used in both the standard-resin and in the toughened-resin composites, the increase in wear rate is assumed to be a resin-controlled property. The toughened-resin systems have been modified to increase their resistance to impact damage, and consequently they are more energy absorbent and ductile than the 5208 standard resin. However, because of this characteristic, these materials wear faster under identical test conditions.

Effect of surface texture.- The effect of varying the surface texture on the wear rates of the six materials tested is shown in figure 10. Each data point is the average of two or three individual test runs, and a least-squares linear curve fit was derived. The curves indicate wear rate was linearly dependent on surface texture; however, the response was not highly sensitive to increases in surface texture in the range tested. Aluminum appears to have the least dependence on texture and the lowest wear rate by an order of magnitude. The curves of the composite materials tested have a slightly higher gradient, with the standard graphite-epoxy material exhibiting the lowest wear rates of the composite materials under the test conditions. Previous investigations on aluminum and other metallic materials showed that wear increased rapidly at texture depths of 0 to 0.006 in.; for texture depths greater than 0.006 in., the gradient of wear rate versus texture increased only slightly for most metallic materials (refs. 6 to 8). The texture range in the present investigation (0.01 to 0.02 in.) is well above the 0.006-in. transition point, and the results agree with trends discussed in previous studies.

Effect of belt velocity.- Results of the abrasion tests performed at belt velocities of 16.0, 36.4, 52.0, and 68.0 mph are shown in figure 11. The data points at 16.0, 36.4, and 52.0 mph represent the average of two or three individual test runs. A single test was run at the 68.0-mph velocity. A least-squares linear curve fit was used to obtain the line through the points as before. The curves indicate a linear relationship between wear rate and belt velocity.

Nathan and Jones (ref. 7) found that the wear of aluminum was not particularly sensitive to velocity. Their experiments were performed on finely textured abrasive-grit paper at much lower velocities and pressures. Figure 11 shows that aluminum

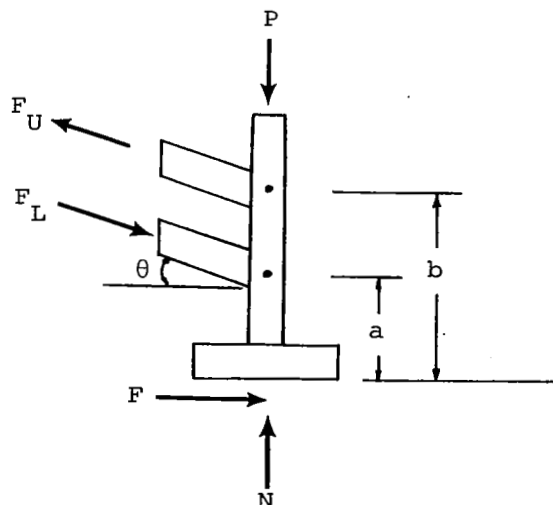
had a much lower wear rate than the composite materials tested for a given velocity. Also, in agreement with the findings of Nathan and Jones, the aluminum wear rate as a function of velocity has a much lower gradient than that of the composite materials. The gradient of the curves for each of the composite materials is approximately the same and, as in the previous tests, the standard graphite-epoxy composites showed less wear than the toughened-resin composites at each velocity.

Effect of fiber orientation.- Results of the tests to determine the effect of fiber orientation on wear rate in composite materials are shown in figure 12. The data show that the least wear occurred when the fibers were parallel (0°) to the sliding direction, and the greatest wear occurred when the fibers were transverse (90°) to the sliding direction. Wear rate increased linearly with angle of orientation between the two extremes.

A study in which the effect of orientation on the wear of carbon-fiber reinforced polyester resin sliding against hardened tool steel (ref. 9) found the greatest wear occurred when the carbon fibers were oriented parallel to the sliding direction. These results are exactly opposite to the results obtained in this investigation. The difference in the findings may be explained by the choice of sliding surfaces. The wear of graphite-epoxy composites against hardened tool steel may occur by different wear and abrasion modes, than wear against very coarse aluminum oxide material, and therefore a comparison between the results of the two investigations probably should not be attempted.

Coefficient-of-Friction Data

The frictional forces developed between the test specimen and the sliding abrasive surface were calculated from a static analysis of the specimen holder (sketched below) given the applied load P , the angle of inclination of the linkage arms θ , and the force output measured from the load cell F_L . Typical force traces from the load cell for the six test materials under identical test conditions are shown in figure 13. The coefficient of friction μ is derived from the computed frictional force based on the measured force in the lower linkage arm.



$$F = F_L (\cos \theta) \left(\frac{a}{b} - 1 \right)$$

$$N = P + F_L (\sin \theta) \left(1 - \frac{a}{b} \right)$$

$$\mu = \frac{F}{N} = \frac{F_L (\cos \theta) \left(\frac{a}{b} - 1 \right)}{P + F_L (\sin \theta) \left(1 - \frac{a}{b} \right)}$$

Plots of the coefficient of friction as a function of pressure, of surface texture, and of velocity are shown in figure 14 for each of the six test materials. There are only slight variations in coefficient of friction with any of the test variables. The data from each of these tests were used to compute an average coefficient of friction for each of the test materials. These average values are shown as a bar chart in figure 15. Aluminum exhibited the highest coefficient of friction, approximately 0.20. The standard graphite-epoxy composite, however, had an average coefficient of friction of about half that value. Kevlar and the toughened-resin composites had somewhat higher coefficients of friction than the standard graphite-epoxy, though not as high as aluminum. These data imply that under the conditions of an airplane belly landing, a transport with a standard graphite-epoxy composite skin could slide twice as far as a similar transport with an aluminum skin, and consequent wear would be several times greater.

Temperature Data

Temperature variation during the abrading process was obtained by averaging the four temperatures measured with the thermocouples imbedded into the test specimens. (See fig. 16.) Specimens were abraded for approximately 20 sec and temperature readings were taken every 4 sec. The increase in temperature with time for these tests was highly nonlinear and is a function of several factors, including the coefficient of friction, the conductivity of the specimen material, and the specimen wear rate. The wear rate is important because the source of heat, which is the friction developed at the contact surface, was constantly moving closer to the thermocouples as the test progressed.

Figure 16 shows that the aluminum reached the highest temperature, approximately 180°F, during a 16-sec run and had the greatest rate of increase in temperature with time. The T300/BP-907, Kevlar 49/934, and T300/Ciba 4 materials had a temperature-time response similar to the aluminum, though their maximum temperatures reached during the test run were not as high (approximately 140°F). The T300/Fibredux 920 and T300/5208 materials heated at a slower rate, and the maximum temperatures attained after 16 sec of abrasion were considerably lower than the aluminum. It should be noted that the temperatures reached by the composite materials after 16 sec of abrasion were approximately half their normal cure temperature. Also, the major temperature increase for all the test materials occurred after about 8 sec of abrasion. The test specimens in the previous tests were abraded for approximately 5 sec, thus falling in the constant temperature range. Consequently, the results of the previous tests should not have been influenced by possible temperature effects.

CONCLUDING REMARKS

The objective of this investigation was to compare the friction and wear response of aluminum and composite materials when subjected to loading conditions similar to those experienced by the skin panels on the underside of a transport airplane during an emergency sliding landing on a runway surface. A laboratory experiment was developed to simulate these conditions. Four types of materials (aluminum, standard graphite-epoxy composite, aramid-epoxy composite, and toughened-resin composites) were used to fabricate small skin test specimens. The specimens were abraded under conditions of varying pressure, surface texture, surface velocity, and fiber orientation. In addition, thermocouples were imbedded in the specimens to obtain a temperature-time history during abrasion.

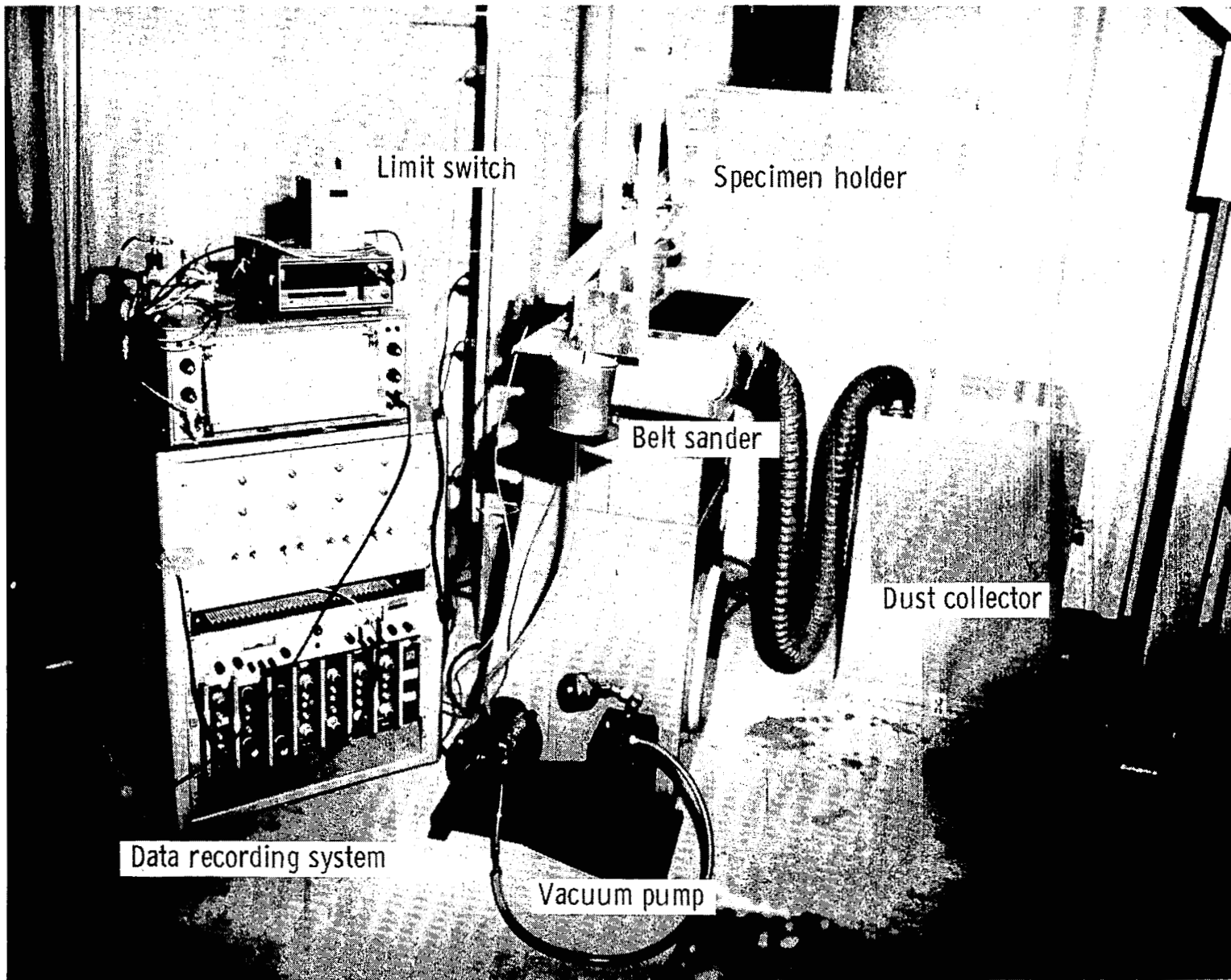
Comparisons between the behaviors of the various materials were made based on wear rates, coefficient-of-friction data, and temperature responses. Major findings of this investigation include:

1. Wear rate for both the aluminum and the composite materials was a linear function of pressure, velocity, and surface texture.
2. In composite materials, wear rate was a linear function of fiber orientation, with the least wear occurring when the fiber direction was parallel to the sliding direction.
3. The coefficient of friction for the standard graphite-epoxy composite was approximately half that for aluminum.
4. Toughened-resin composite materials and aramid-epoxy composite exhibited coefficients of friction of the same magnitude as aluminum, but wore faster than the standard graphite-epoxy composite.
5. The temperature-time response of both the aluminum and the composite materials was highly nonlinear, with aluminum reaching the highest temperature during abrasion for a specified time.

Langley Research Center
National Aeronautics and Space Administration
Hampton, VA 23665
December 12, 1983

REFERENCES

1. Passengers Praise Pilot for Actions in Accident. *Times-Herald* (Newport News, Va.), 83rd year, no. 71, Mar. 24, 1983, p. 13.
2. Williams, Jerry G.; and Rhodes, Marvin D.: The Effect of Resin on the Impact Damage Tolerance of Graphite-Epoxy Laminates. NASA TM-83213, 1981.
3. Leland, Trafford J. W.; Yager, Thomas J.; and Joyner, Upshur T.: Effects of Pavement Texture on Wet-Runway Braking Performance. NASA TN D-4323, 1968.
4. Yager, Thomas J.; Phillips, W. Pelham; Horne, Walter B.; and Sparks, Howard C. (With appendix D by R. W. Sugg): A Comparison of Aircraft and Ground Vehicle Stopping Performance on Dry, Wet, Flooded, Slush-, Snow-, and Ice-Covered Runways. NASA TN D-6098, 1970.
5. Bisson, E. E.: Various Modes of Wear and Their Controlling Factors. Evaluation of Wear Testing, ASTM STP 446, c.1969, pp. 1-22.
6. Liu, Y. J.; Yand, R. L.; Cheng, K. Q.; and Deng, H. J.: Wear of Metallic Materials Under Dynamic Loading. *Wear of Materials - 1981*, S. K. Rhee, A. W. Ruff, and K. C. Ludema, eds., American Soc. Mech. Eng., c.1981, pp. 390-395.
7. Nathan, G. K.; and Jones, W. J. D.: The Empirical Relationship Between Abrasive Wear and the Applied Conditions. *Wear*, vol. 9, no. 4, July-Aug. 1966, pp. 300-309.
8. Finkin, E. F.: Abrasive Wear. Evaluation of Wear Testing, ASTM STP 446, c.1969, pp. 55-90.
9. Buckley, Donald H.: Surface Effects in Adhesion, Friction, Wear, and Lubrication. Elsevier Scientific Pub. Co., 1981.



Limit switch

Specimen holder

Belt sander

Dust collector

Data recording system

Vacuum pump

L-83-1393

Figure 1.- Abrasion test apparatus.

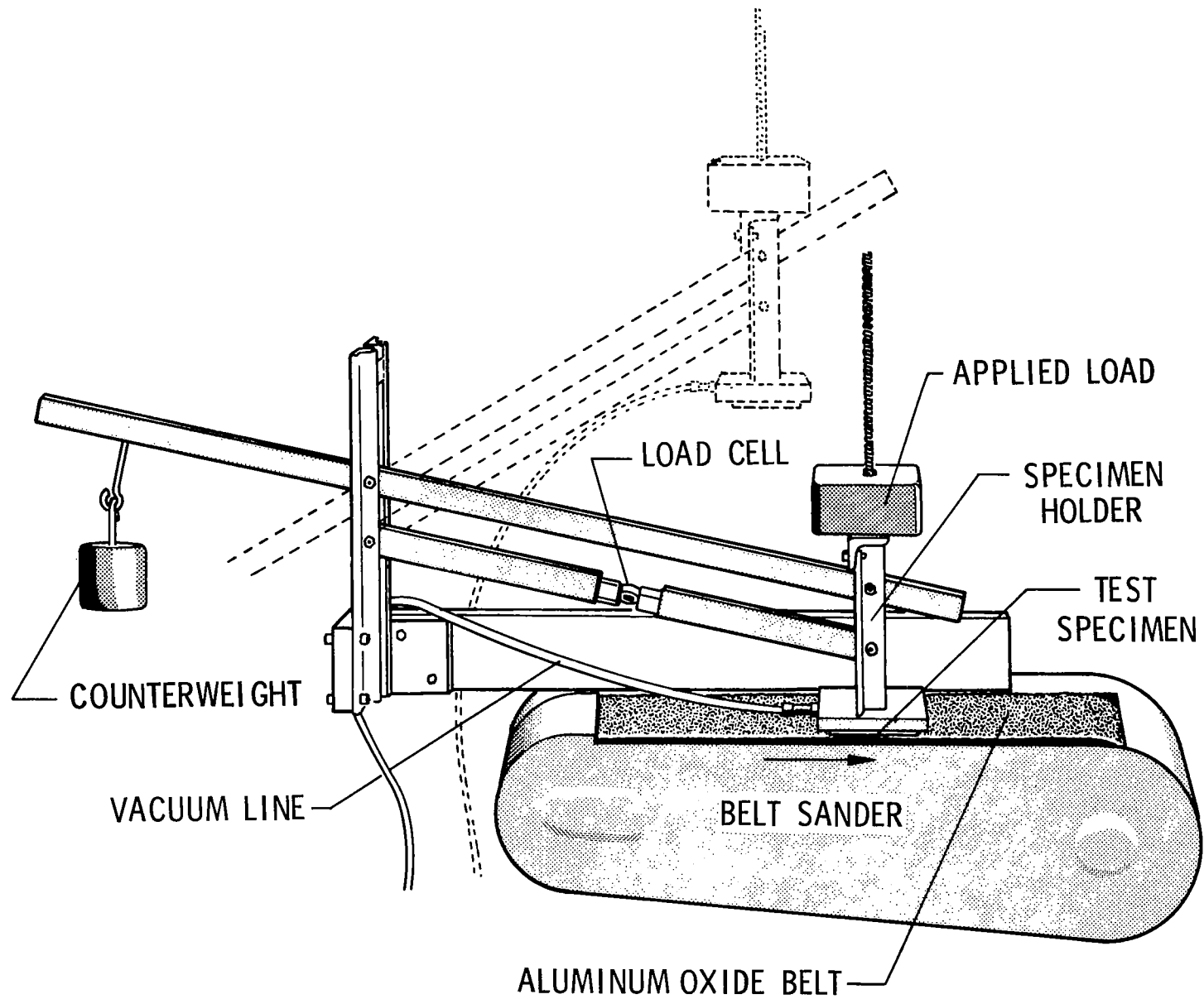
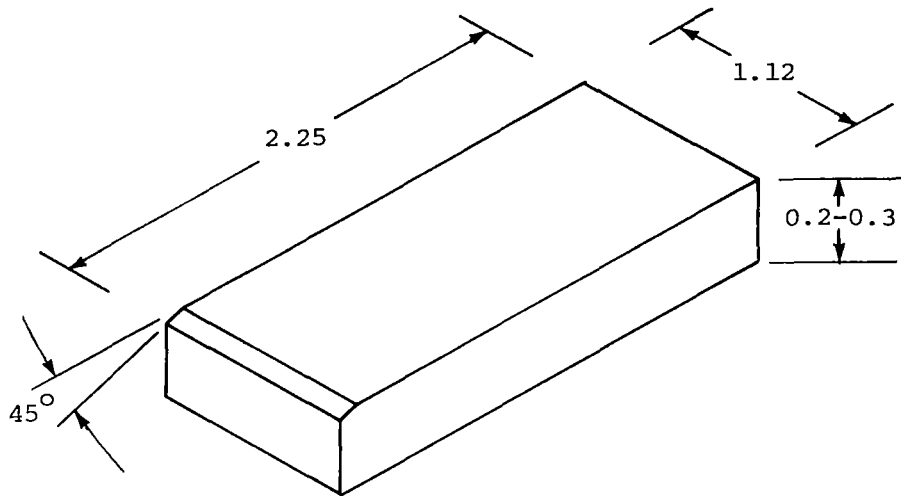


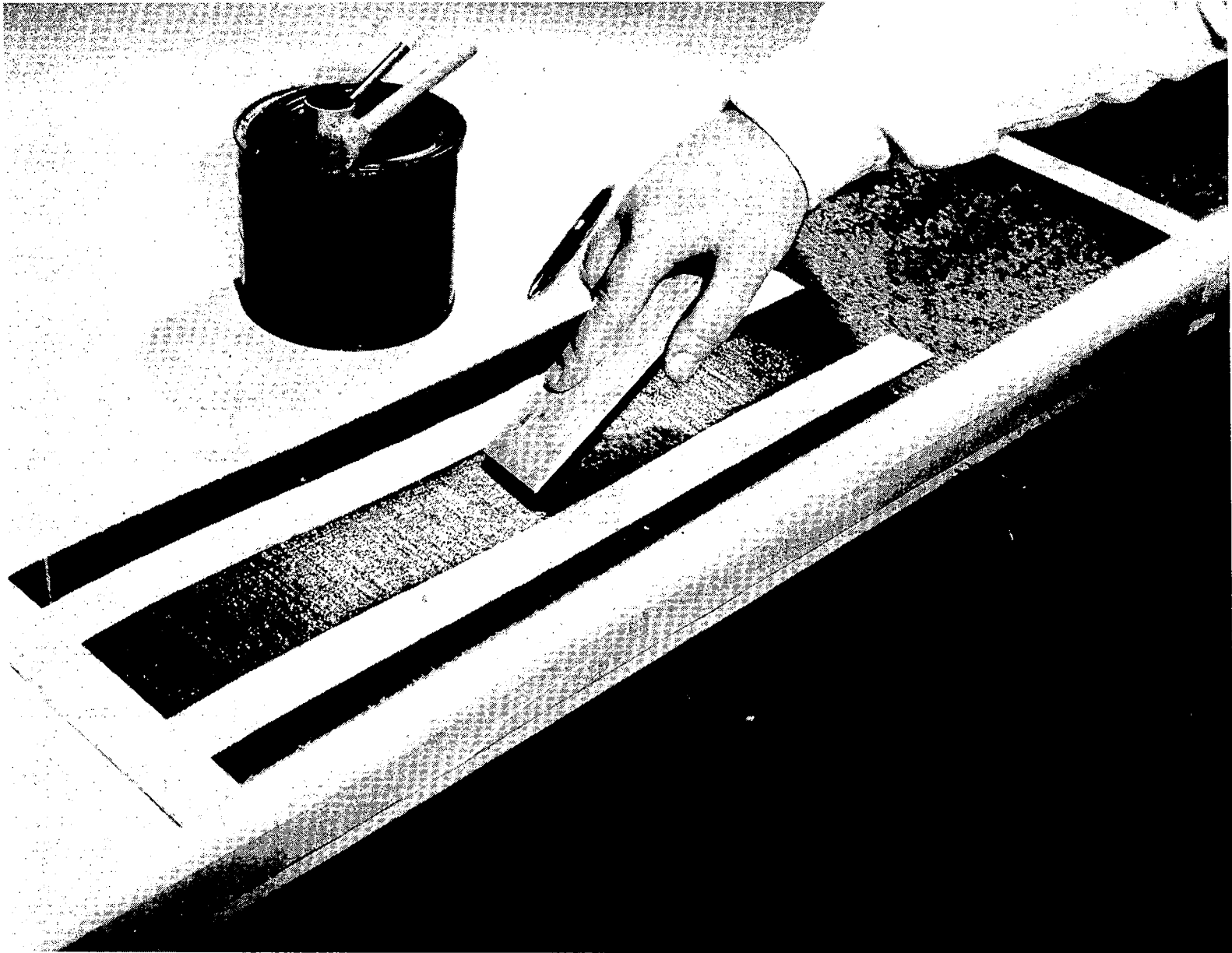
Figure 2.- Schematic drawing of abrasion test apparatus depicting the parallelogram arrangement of the linkage arms.



TEST MATERIALS

Material	Lay-up
Aluminum: 2024-T4	
Composite: T300/5208	$(\underline{+45/0/90}/\bar{+45/0/90})_{3S}$ $(\underline{+45/0}_2/\underline{+45/0}_2/\underline{+45/0/90})_{2S}$
Kevlar 49/934	
T300/BP-907	
T300/Fibredux 920	
T300/Ciba 4	

Figure 3.- Schematic drawing of a typical abrasion specimen and a list of the types of aluminum and composite materials used in abrasion tests. Drawing dimensions are in inches unless otherwise noted.



L-83-2538

Figure 4.- Illustration of grease sample technique to determine texture depth of aluminum oxide grit belts.

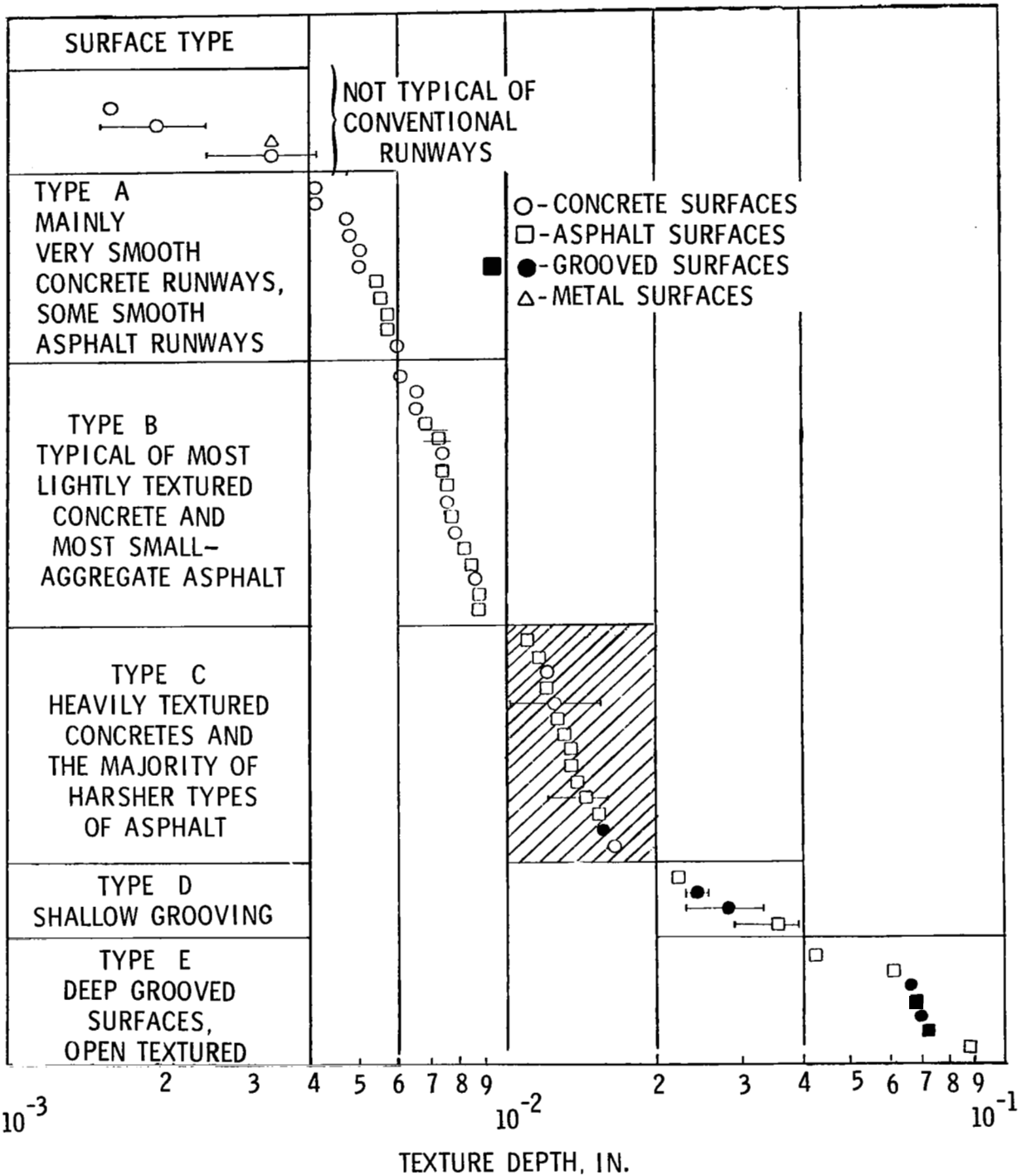


Figure 5.- Classification of runway surfaces. Texture depths measured by grease or sand patch methods. (From data in ref. 4.)

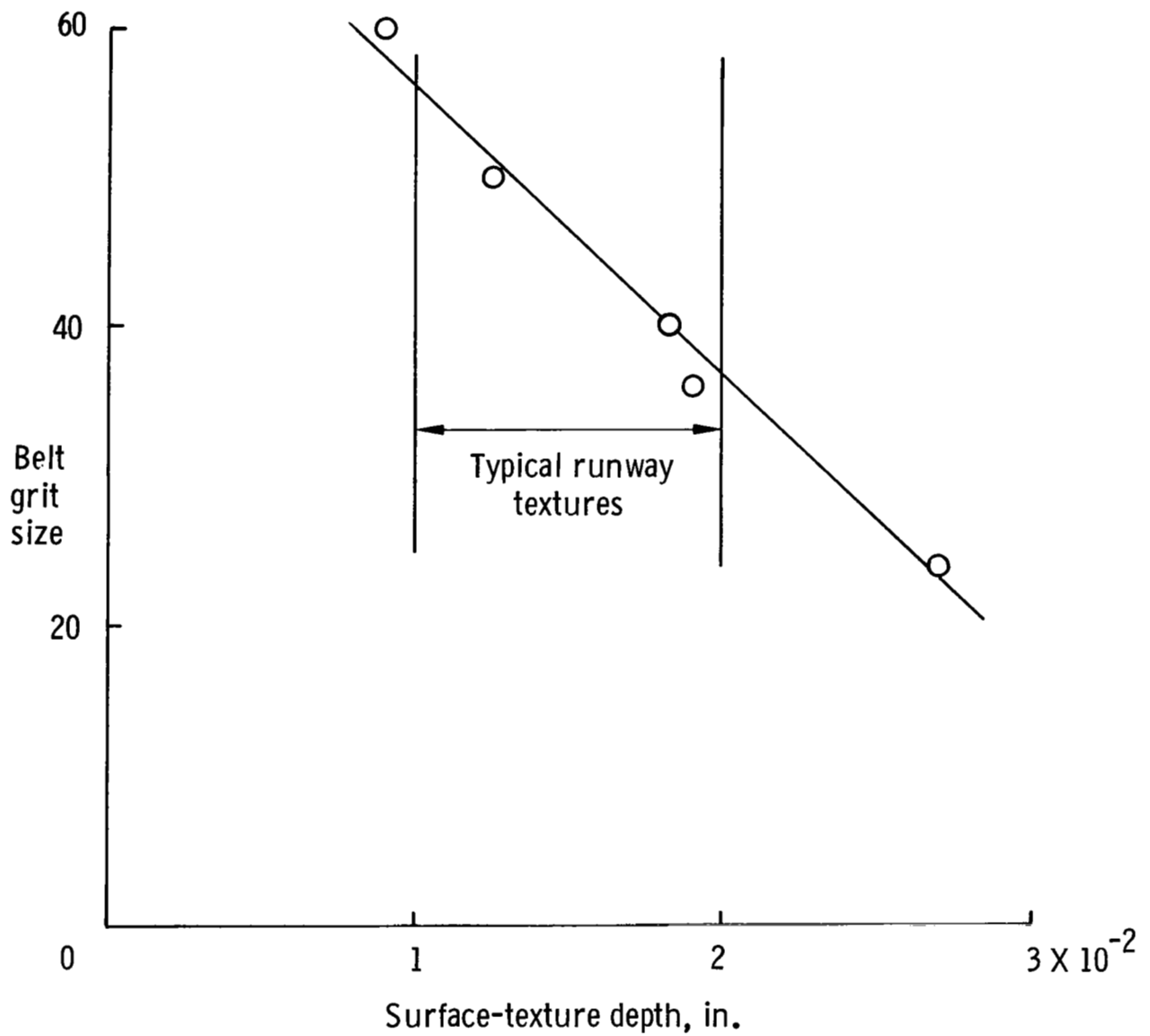
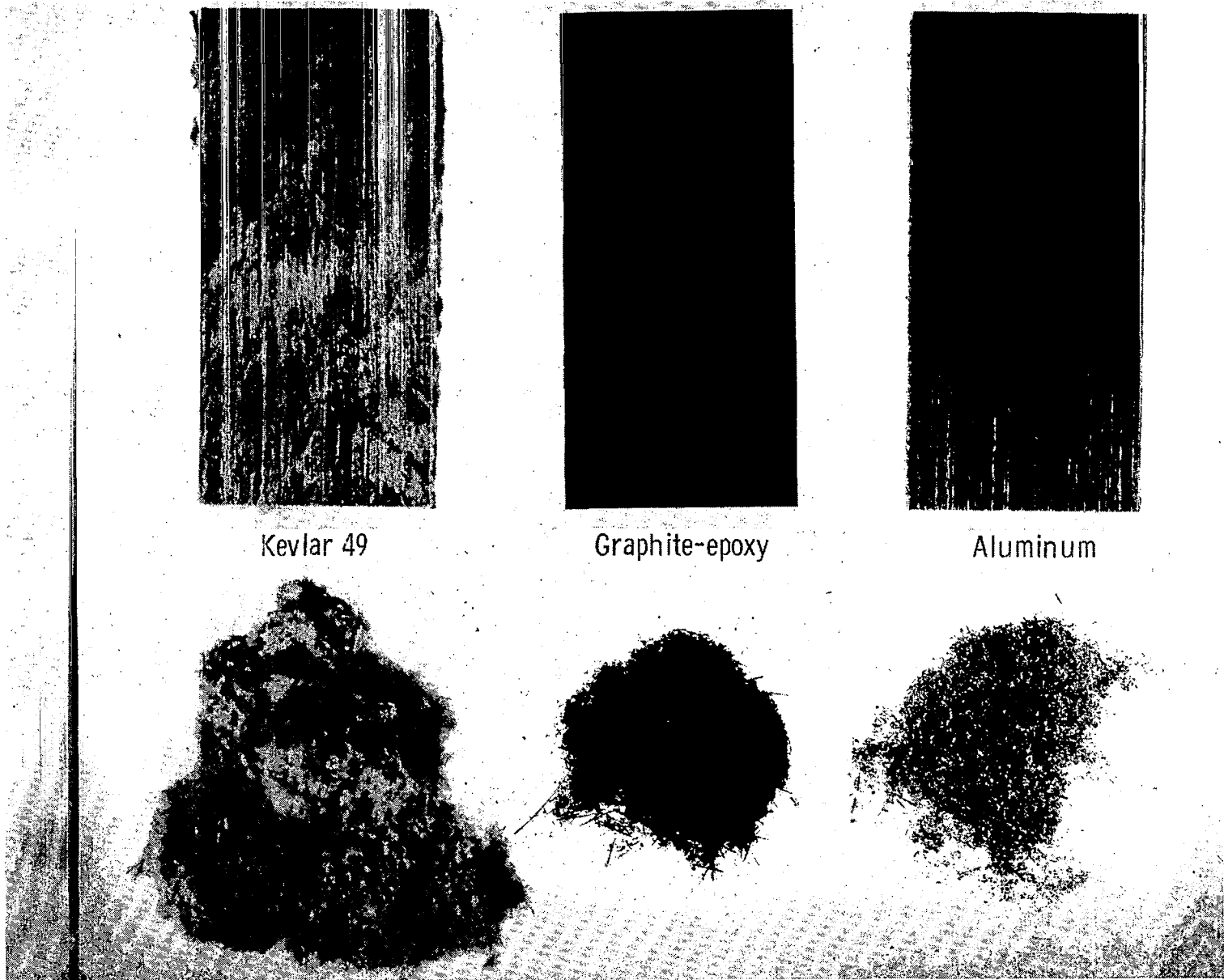


Figure 6.- Results of performing grease sample technique on aluminum oxide belts. Belts lying in the typical range were used in abrasion testing.



L-83-2408

Figure 7.- General appearance of wear surface and wear debris particles for typical Kevlar, graphite-epoxy, and aluminum specimens. Wear debris shown is not indicative of volume of wear for each specimen type.

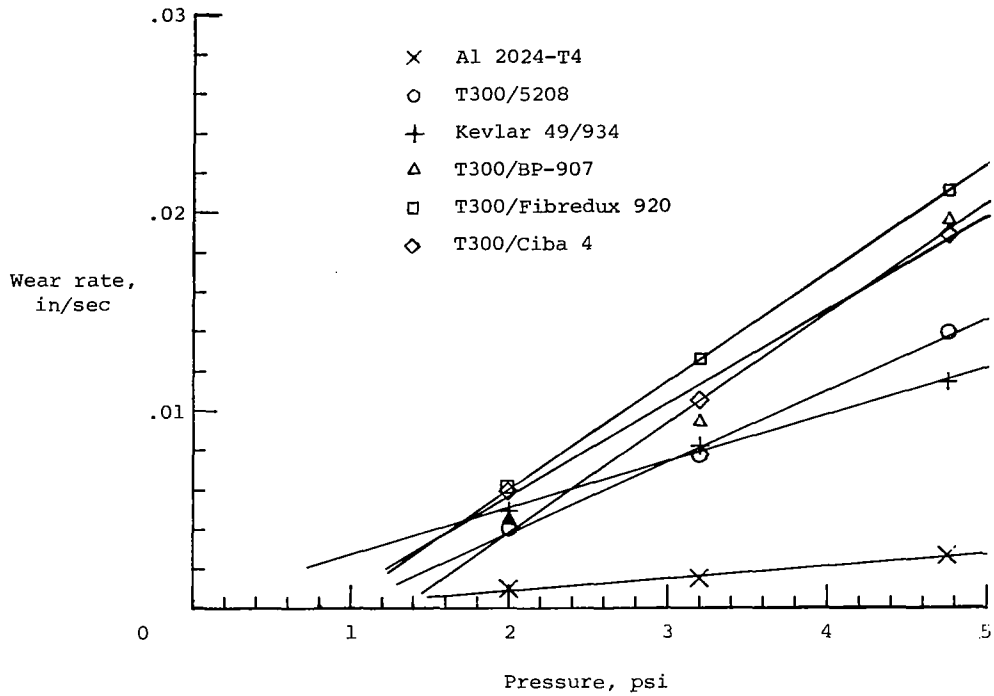


Figure 8.- Wear rate as a function of normal loading at a belt velocity of 36.4 mph for the No. 36 grit belt.

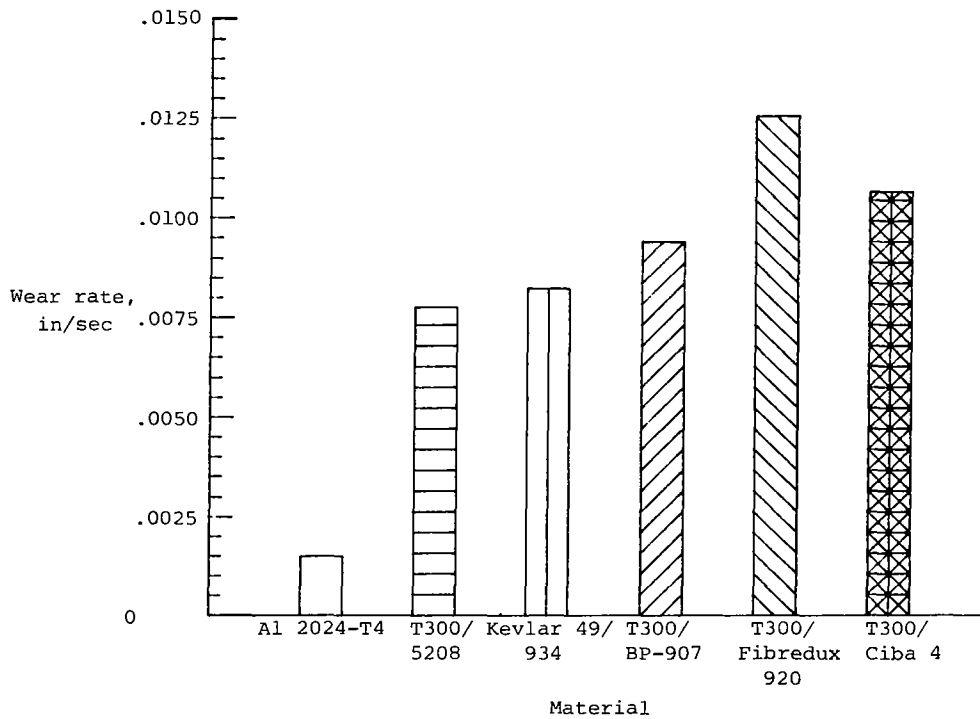


Figure 9.- Comparison of wear rates of test materials at a belt velocity of 36.4 mph for the No. 36 grit belt and a 3.2-psi pressure.

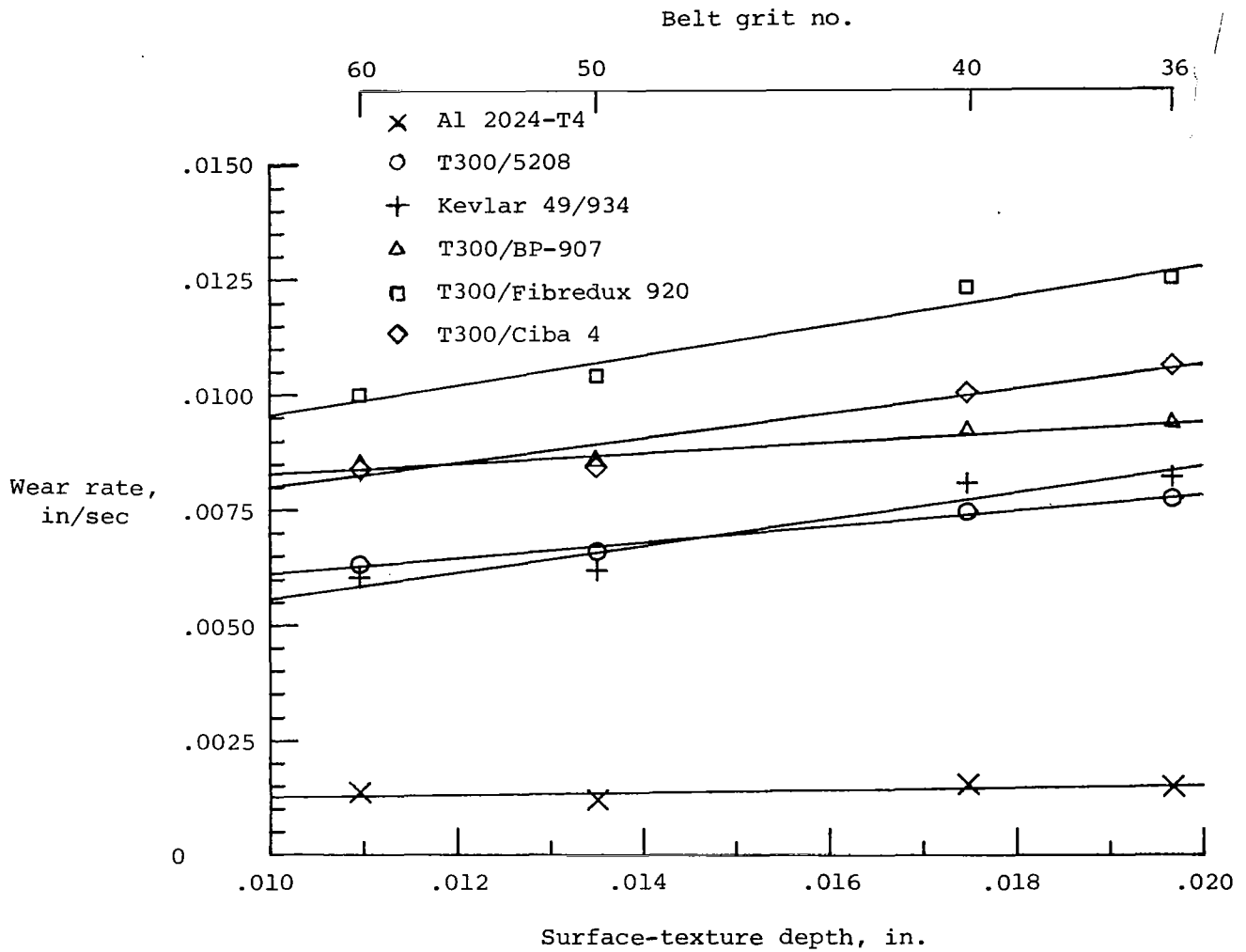


Figure 10.- Wear rate as a function of surface-texture depth for a belt velocity of 36.4 mph and a 3.2-psi pressure.

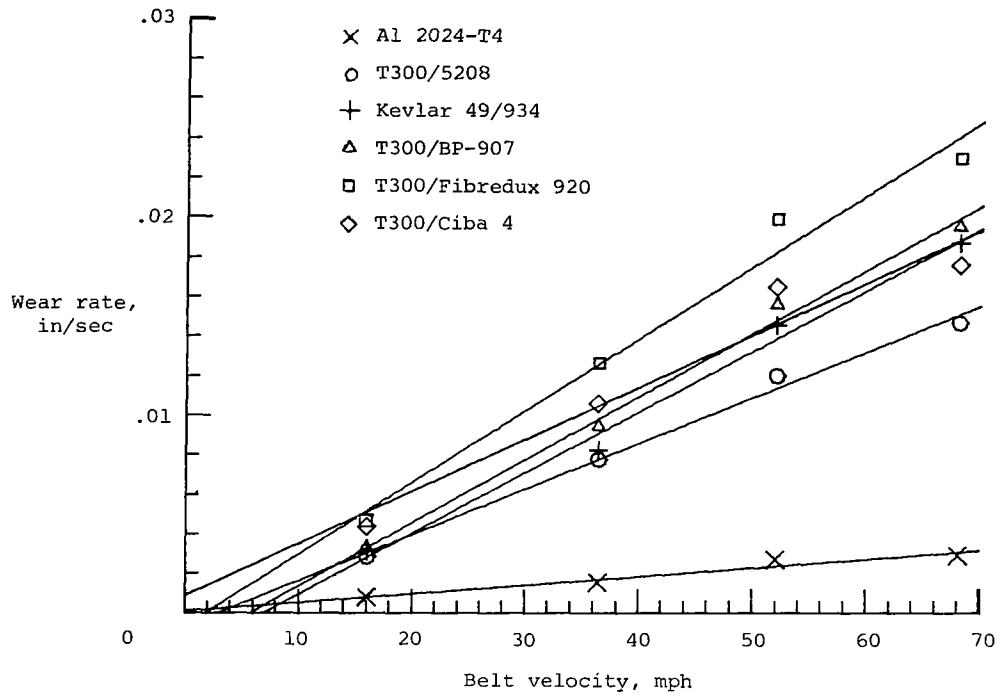


Figure 11.- Wear rate as a function of belt velocity for the No. 36 grit belt and a 3.2-psi pressure.

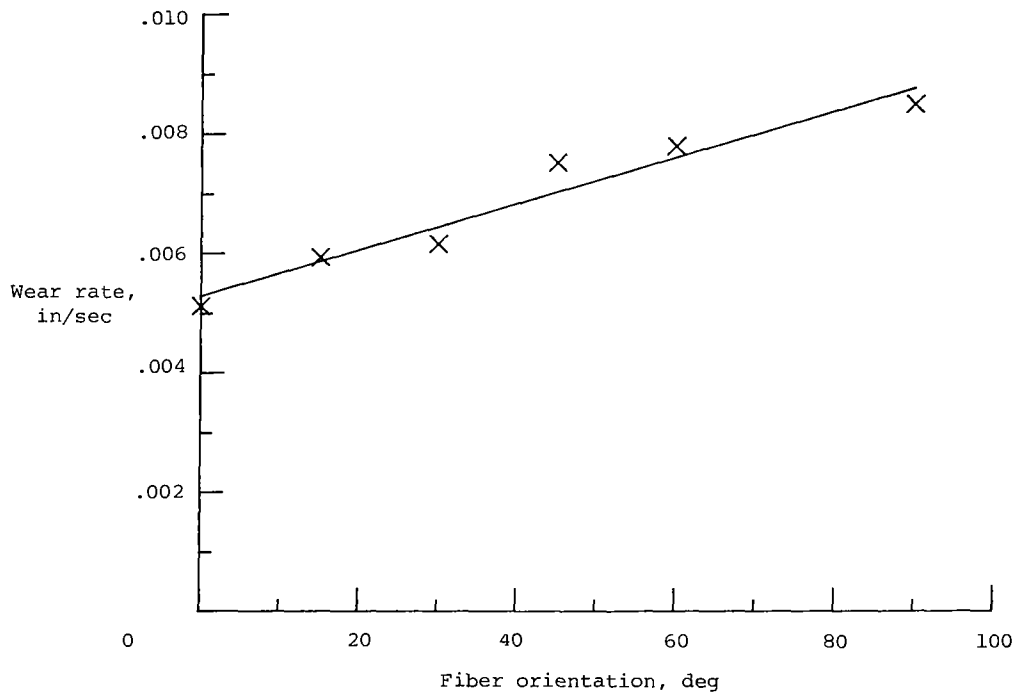


Figure 12.- Wear rate as a function of fiber orientation for AS4/3502 graphite-epoxy composite at a belt velocity of 36.4 mph for the No. 50 grit belt and a 3.2-psi pressure.

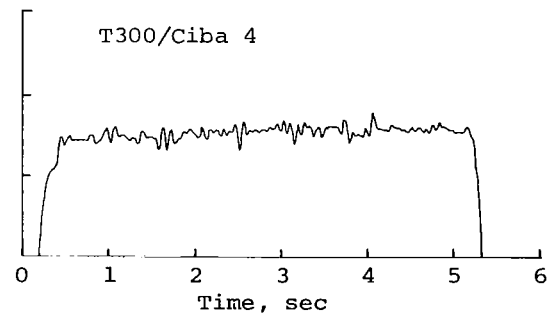
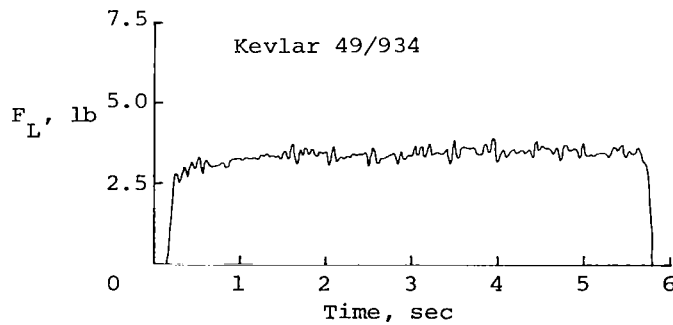
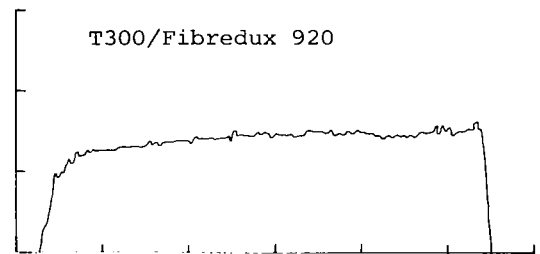
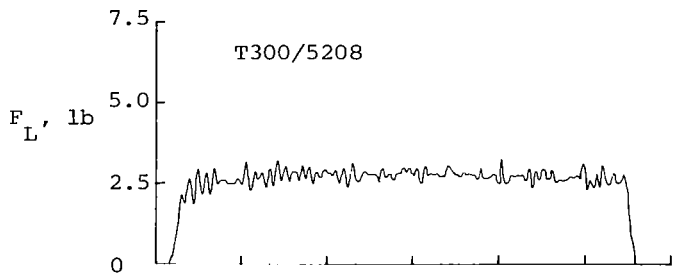
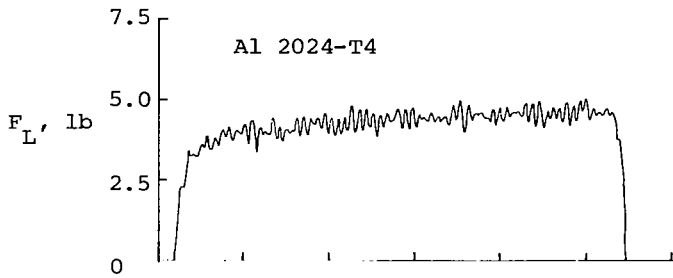


Figure 13.- Force traces from load cell during abrasion test runs at a belt velocity of 36.4 mph for the No. 40 grit belt and a 3.2-psi pressure.

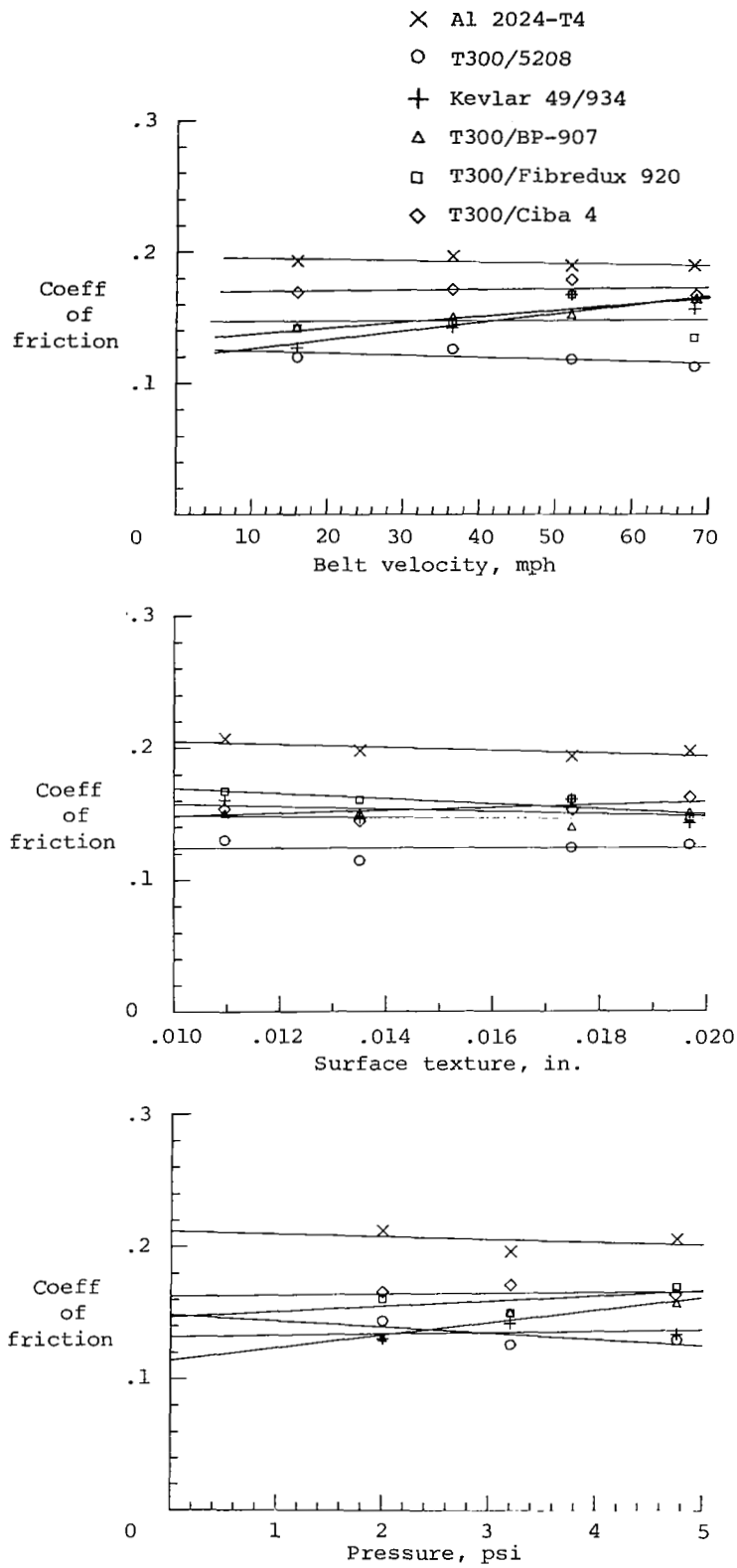


Figure 14.- Coefficient of friction as a function of pressure, of surface texture, and of belt velocity.

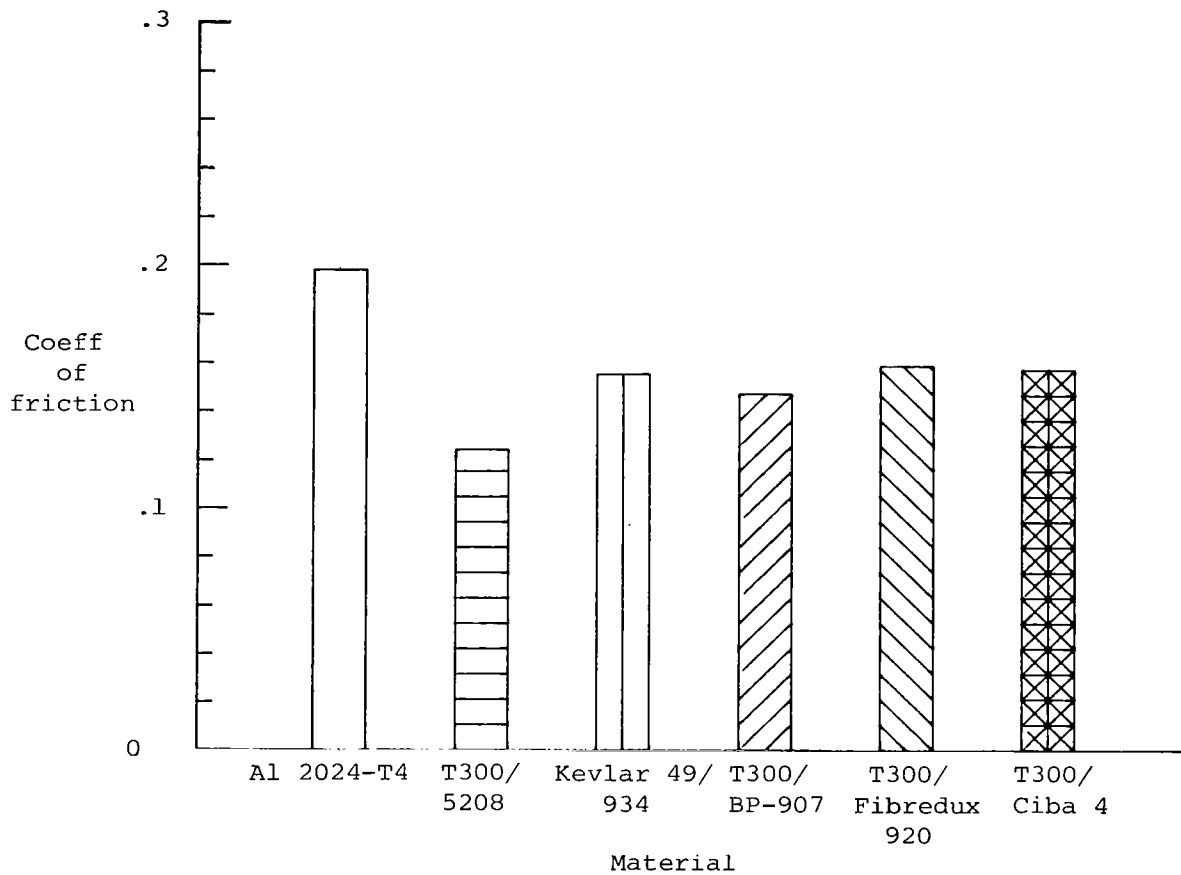


Figure 15.- Average coefficients of friction of six test materials.

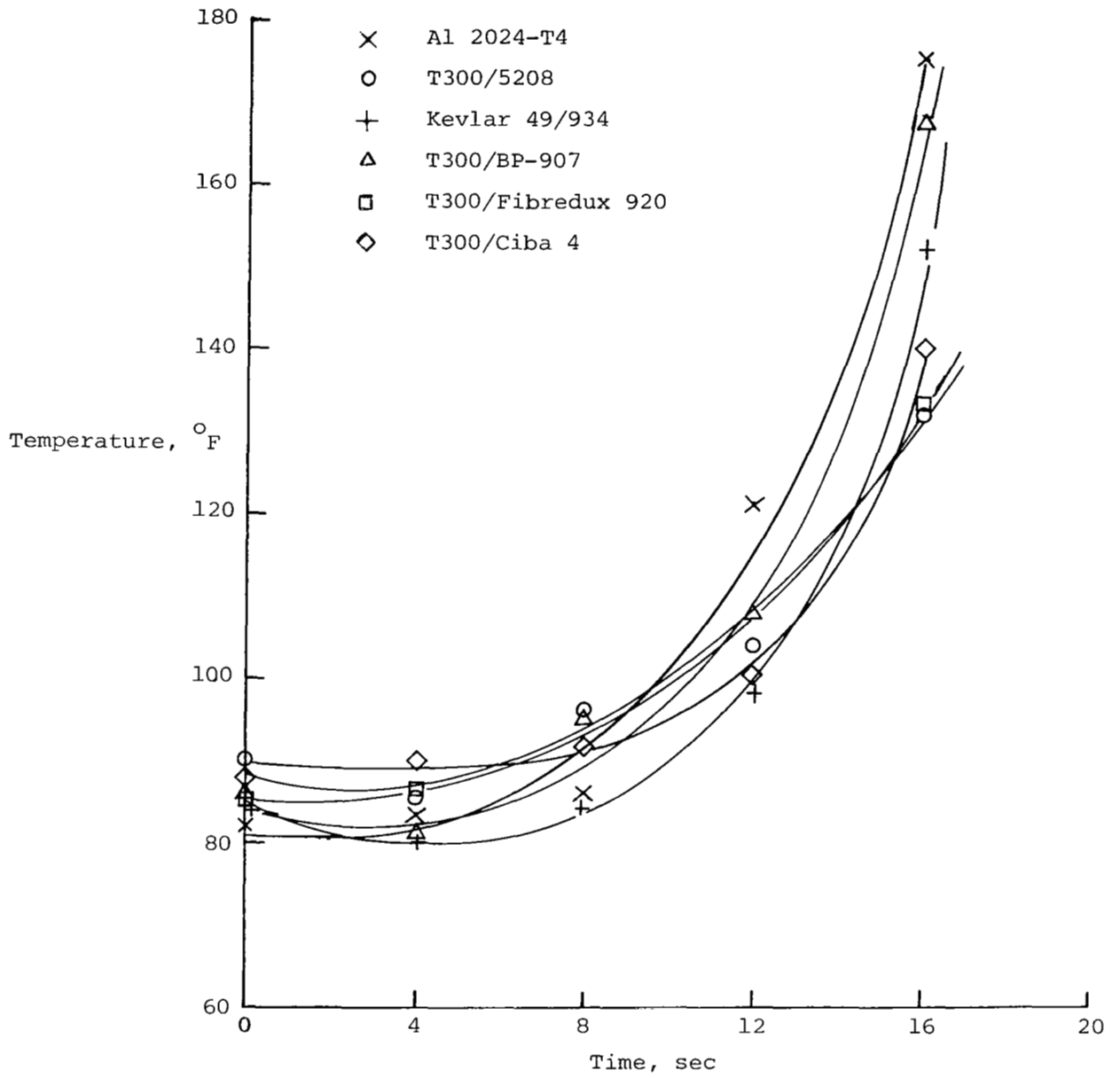


Figure 16.- Temperature as a function of time for six test materials.

1. Report No. NASA TP-2262 AVSCOM TR 83-B-7		2. Government Accession No.		3. Recipient's Catalog No.	
4. Title and Subtitle FRICTION AND WEAR BEHAVIOR OF ALUMINUM AND COMPOSITE AIRPLANE SKINS				5. Report Date February 1984	
				6. Performing Organization Code 505-33-53-09	
7. Author(s) Karen E. Jackson				8. Performing Organization Report No. L-15697	
9. Performing Organization Name and Address Structures Laboratory USAAVSCOM Research and Technology Laboratories NASA Langley Research Center Hampton, VA 23665				10. Work Unit No.	
				11. Contract or Grant No.	
12. Sponsoring Agency Name and Address National Aeronautics and Space Administration Washington, DC 20546 and U.S. Army Aviation Systems Command St. Louis, MO 63166				13. Type of Report and Period Covered Technical Paper	
				14. Army Project No. 1L161102AH45	
15. Supplementary Notes Karen E. Jackson: Structures Laboratory, USAAVSCOM Research and Technology Laboratories.					
16. Abstract Friction and wear behavior was determined for small skin specimens under abrasive loading conditions typical of those occurring on the underside of a transport airplane during an emergency belly landing. A test apparatus consisting of a standard belt sander provided the sliding surface. Small test specimens constructed of aluminum, standard graphite-epoxy composite, aramid-epoxy composite, and toughened-resin composites were tested under a range of pressures, belt velocities, and belt-surface textures. The effects of these test variables on the wear rate and the coefficient of friction are discussed and comparisons are made between the composite materials and aluminum. The effect of fiber orientation in the composite materials on wear rate was also investigated. In addition, tests were performed in which thermocouples were imbedded into the various test specimens to obtain temperature-time histories during abrasion.					
17. Key Words (Suggested by Author(s)) Abrasion of composites Friction and wear of metal and composites Composite airplane skin Toughened-resin composites			18. Distribution Statement Unclassified - Unlimited Subject Category 05		
19. Security Classif. (of this report) Unclassified	20. Security Classif. (of this page) Unclassified	21. No. of Pages 26	22. Price* A03		